

A technical study of Chinese Buddhist sculptures: first insights into a complex history of transformation through analysis of the polychrome decoration

Original

A technical study of Chinese Buddhist sculptures: first insights into a complex history of transformation through analysis of the polychrome decoration / Ricci, Chiara; Buscaglia, Paola; Angelici, Debora; Piccirillo, Anna; Matteucci, Enrica; Demonte, Daniele; Tasso, Valentina; Sanna, Noemi; Zenucchini, Francesca; Croci, Sara; Di Iorio, Federico; Vigo, Laura; Quadrio, Davide; Pozzi, Federica. - In: COATINGS. - ISSN 2079-6412. - ELETTRONICO. - 14:3(2024).
[10.3390/coatings14030344]

Availability:

This version is available at: 11583/2986964 since: 2024-03-14T15:33:34Z

Publisher:

MDPI

Published

DOI:10.3390/coatings14030344

Terms of use:








This article is made available under terms and conditions as specified in the corresponding bibliographic description in the repository

Publisher copyright

(Article begins on next page)

Article

A Technical Study of Chinese Buddhist Sculptures: First Insights into a Complex History of Transformation through Analysis of the Polychrome Decoration

Chiara Ricci ^{1,*} , Paola Buscaglia ^{1,2}, Debora Angelici ¹, Anna Piccirillo ¹ , Enrica Matteucci ¹ ,
Daniele Demonte ¹, Valentina Tasso ¹, Noemi Sanna ^{1,3} , Francesca Zenucchini ¹, Sara Croci ², Federico Di Iorio ² ,
Laura Vigo ⁴ , Davide Quadrio ⁵ and Federica Pozzi ¹ 

¹ Centro per la Conservazione ed il Restauro dei Beni Culturali “La Venaria Reale”, 10078 Venaria Reale (Turin), Italy; paola.buscaglia@ccrvenaria.it (P.B.); anna.piccirillo@ccrvenaria.it (A.P.); enrica.matteucci@ccrvenaria.it (E.M.); daniele.demonte@ccrvenaria.it (D.D.); valentina.tasso@ccrvenaria.it (V.T.); francesca.zenucchini@ccrvenaria.it (F.Z.); federica.pozzi@ccrvenaria.it (F.P.)

² Dipartimento di Scienza Applicata e Tecnologia, Politecnico di Torino, 10129 Turin, Italy; paola.buscaglia@polito.it (P.B.); sara.croci@polito.it (S.C.); federico.diiorio@polito.it (F.D.I.)

³ Dipartimento di Scienze dell’Antichità, Università degli Studi di Roma “La Sapienza”, 00185 Rome, Italy; noemi.sanna@uniroma1.it

⁴ Montreal Museum of Fine Arts, Montreal, QC H3G 1J5, Canada; lvigo@mbamtl.org

⁵ Museo d’Arte Orientale (MAO), 10122 Turin, Italy; davide.quadrio@fondazionetorinomusei.it

* Correspondence: chiara.ricci@ccrvenaria.it; Tel.: +39-011-4993021

Abstract: Artifacts pertaining to Buddhist culture are often studied in relation to their circulation from India throughout the rest of Asia; however, many traveled to Europe during the last few centuries as trade commodities and pieces for the art market, losing any devotional purpose in favor of a specific aesthetic sensitivity that was typically adapted to Western taste to appeal to collectors. This article presents a technical study of seven polychrome wooden sculptures from the Museo d’Arte Orientale (MAO) in Turin, Italy. Originally from China, these objects are generally attributed to the late Ming–early Qing dynasties (16th–18th centuries) based merely on stylistic and iconographic considerations. Scientific analysis sought to expand the available knowledge on their constituting materials and fabrication techniques, to address questions on their authenticity, to assess their state of preservation, and to trace the history of transformations they have undergone while transitioning from devotional objects to private collection and museum artwork. By delving into the sculptures’ intricate paint stratigraphy, the results were also key to guiding treatment choices. The outcomes of this study were featured in the MAO exhibition “Buddha10. A Fragmented Display on Buddhist Visual Evolution” (October 2022–September 2023).

Keywords: Chinese artifacts; Buddha; devotional objects; wooden sculptures; polychromy; paint layers; repainting; Museo d’Arte Orientale (MAO); technical study



Citation: Ricci, C.; Buscaglia, P.; Angelici, D.; Piccirillo, A.; Matteucci, E.; Demonte, D.; Tasso, V.; Sanna, N.; Zenucchini, F.; Croci, S.; et al. A Technical Study of Chinese Buddhist Sculptures: First Insights into a Complex History of Transformation through Analysis of the Polychrome Decoration. *Coatings* **2024**, *14*, 344. <https://doi.org/10.3390/coatings14030344>

Academic Editor: Marko Petric

Received: 2 February 2024

Revised: 8 March 2024

Accepted: 12 March 2024

Published: 13 March 2024



Copyright: © 2024 by the authors. Licensee MDPI, Basel, Switzerland. This article is an open access article distributed under the terms and conditions of the Creative Commons Attribution (CC BY) license (<https://creativecommons.org/licenses/by/4.0/>).

1. Introduction

Objects pertaining to Buddhist visual and material culture are often studied in relation to their circulation from India throughout the rest of Asia, while, to date, little attention has been paid to understanding their westward migration even though numerous examples are currently preserved in both public and private collections in Europe and the United States. Originating from different geographical areas and cultural contexts within the Asian continent, many of these artifacts traveled to Europe during the last few centuries to be sold as trade commodities and pieces for the art market. As a result of this transition, they lost any devotional value or purpose in favor of a specific aesthetic sensitivity that was typically adapted to Western taste to appeal to collectors.

This contribution focuses on a selection of seven polychrome wooden sculptures from the Museo d'Arte Orientale (MAO) in Turin, Italy, which have recently undergone an in-depth technical study and conservation treatment at the Centro per la Conservazione ed il Restauro dei Beni Culturali (CCR) "La Venaria Reale" (Figure 1). These objects, never exhibited until recent times, are generally described in the museum entries as being of Chinese origin, specifically from the late Ming–early Qing dynasties (16th–18th centuries), based merely on stylistic and iconographic considerations.



Figure 1. Object of this study. Selection of seven Buddhist polychrome wooden sculptures from the Museo d'Arte Orientale (MAO) in Turin, Italy, analyzed in this technical study.

While Japanese Buddhist sculpture has been the subject of more extensive art historical and scientific studies [1–6], Chinese production related specifically to the type of artifacts in this article constitutes, to date, an understudied field in need of further dedicated research. Previous investigations of Chinese Buddhist sculpture have focused, for instance, on the polychromy of stone and clay figures from various temple locations [7–11], as well as on a relevant body of copper-alloy statues in the collection of the Freer Gallery of Art (Washington, DC, USA) [12]. In terms of polychrome wooden artifacts, the literature reports technical studies of 11th to 12th century Guanyin sculptures from the Isabella Stewart Gardner Museum (Boston, US) [13] and the Nelson-Atkins Museum of Art (Kansas City, MO, USA) [14], whose surfaces show a similar combination of partial losses and non-contemporary paints that attest to a complex history of repair and redecoration in accordance with evolving tastes in statuary. In addition, the Royal Ontario Museum (Toronto, ON, Canada) carried out a scientific study regarding the Chinese polychrome sculptures in their holdings as part of a broader survey on Asian sculptural arts [15], and further work on the examination and treatment of such objects was conducted at the Victoria and Albert Museum (London, UK) [16,17], the Rijksmuseum (Amsterdam, The Netherlands) [18], and The Metropolitan Museum of Art (New York, NY, USA) [19].

In this context, the present work sought primarily to fill in the gaps regarding the sculptures' materials and fabrication techniques, ultimately aiming to discriminate any extant paint layers belonging to the original decoration from the later repainting applied as the objects were transferred to Europe. Data from the technical investigations were used to verify the current theories related to their authenticity and time of production. A thorough evaluation of the artifacts' state of preservation was also performed based on materials analysis. Not only did the results contribute to an improved understanding of this type of Chinese sculpture, but they also played a crucial role in guiding CCR conservators in their treatment choices. Overall, the wealth of information unveiled by this interdisciplinary endeavor was key to tracing the complex history of transformation that the present selection of MAO sculptures have undergone while transitioning from devotional objects to private collection artworks and museum holdings. The methodological approach adopted relied on

a close and fruitful exchange between scientists, conservators, and Buddhist art specialists, aiming to balance treatment goals in consideration of both European and traditional Asian perspectives. The outcomes of this study were featured in the “Buddha10. A Fragmented Display on Buddhist Visual Evolution” exhibition, held at the MAO from October 2022 to September 2023. In this context, the museum requested to have all the artifacts treated except for Inv. 450, which is iconographically specular to Inv. 451. This choice aimed to provide the public with a direct comparison between a figure that has undergone conservation and its untreated twin, whose surface was thoroughly documented through a 3D multispectral model. Some of the conservation work was carried out in the exhibition space, providing visitors with a unique opportunity to witness this delicate process firsthand.

2. Materials and Methods

The seven polychrome wooden sculptures in this study, belonging to the collection of MAO in Turin, Italy, represent different Buddha manifestations and followers of Gautama. Originally conceived for temple areas with an indoor placement, they served the devotional purpose of guiding devotees in their meditation process. The selection under investigation includes the following subjects: three Lohan or Arhat (Inv. 448, Fujian region, 16th century; Inv. 449, Sichuan region, likely 18th century; Inv. 454, China, exact provenance unknown, 16th century), representing the followers of Gautama Buddha who attained the four progressive stages of enlightenment culminating in full awakening; two Bodhisattva (Inv. 450 and Inv. 451, Shanxi or Shaanxi region, 16th century), namely individuals on the path to awakening; one Guanyin (Inv. 453, Shanxi or Shaanxi region, 17th century), representing a Bodhisattva associated with compassion; and one Buddha (Inv. 452, Shanxi or Shaanxi region, 16th century), i.e., the one who has awakened from the deep sleep of ignorance and has opened his consciousness to encompass all objects of knowledge.

The analytical protocol entailed the use of non-invasive imaging and point techniques, followed by sampling and micro-invasive investigations. Visible diffuse light photography and multiband imaging sought to gather preliminary information on the distribution of various materials on the objects’ surface. Fiber optics reflectance spectroscopy (FORS), X-ray fluorescence (XRF) spectroscopy, and Raman spectroscopy were used jointly to characterize the color palette non-invasively. Overall, 72 microscopic samples, including 46 loose scrapings and 26 multi-layered specimens, were removed from select areas of interest and analyzed through transmission Fourier-transform infrared (FTIR) spectroscopy, optical microscopy, and scanning electron microscopy coupled with energy-dispersive X-ray spectroscopy (SEM/EDS) to complete materials identification, shed light on the paint stratigraphy, and evaluate any ongoing degradation phenomena. Further details on the instrumentation and experimental settings employed are reported below.

Visible diffuse light photography. Lighting was achieved with two Elinchrom RX1200 strobes located to the right and left of the object, at an angle of approximately 45° to the normal to the surface, and with the aid of softboxes to diffuse the light. Photographs were taken with a Nikon D810 DSLR Full Spectrum camera, modified to extend its spectral sensitivity in the 350–1000 nm range and providing a resolution of 7360 × 4912 pixels, equipped with a complementary metal oxide semiconductor (CMOS) silicon sensor as well as Madatec UV-IR Cut and BG40 filters. Image processing, carried out in Adobe Photoshop 25.3.1, included a color correction step conducted by inserting a 24-color X-Rite ColorChecker Classic reference in the field of view.

Infrared reflectography (IRR) and false color processing (IRFC). Lighting was achieved with two Elinchrom RX1200 strobes located to the right and left of the object, at an angle of approximately 45° to the normal to the surface, and with the aid of softboxes to diffuse the light. Photographs were taken with a Nikon D810 DSLR Full Spectrum camera, modified to extend its spectral sensitivity in the 350–1000 nm range and providing a resolution of 7360 × 4912 pixels, equipped with a CMOS silicon sensor as well as a Madatec IR 850 filter.

IRFC images were obtained in the RGB color space of Adobe Photoshop by using two reflection images acquired in the visible and near-IR (NIR) spectral ranges. In particular, the green (G) and red (R) components of the visible image are transferred into the blue (B) and green (G) channels, while the red (R) component is replaced with the NIR image. This methodology yields false color images of the NIR-R-G (RGB) type.

Ultraviolet-induced visible fluorescence (UVF). Lighting was achieved with two Elinchrom RX1200 strobes equipped with a B + W 403 filter by moving the lights at different angles at constant distance. The acquisition involved taking several shots on the same frame by setting the camera to 'Multiple Exposure' to merge illuminations from different positions. Photographs were taken with a Nikon D810 DSLR Full Spectrum camera, modified to extend its spectral sensitivity in the 350–1000 nm range and providing a resolution of 7360×4912 pixels, equipped with a CMOS silicon sensor as well as Madatec UV-IR Cut and BG40 filters. Image processing, carried out in Adobe Photoshop 25.3.1, was conducted by inserting a non-fluorescent reference in the field of view.

Visible-induced infrared luminescence (VIL). Lighting was achieved with a Nikon SB-910 portable speedlight, equipped with 3 Hoya UV-IR Cut filters. The acquisition involved taking several shots on the same frame by setting the camera to 'Multiple Exposure' to merge illuminations from different positions. Images were acquired in the 850–1000 nm spectral range with a Nikon D810 DSLR Full Spectrum camera, modified to extend its spectral sensitivity in the 350–1000 nm range and providing a resolution of 7360×4912 pixels, equipped with a CMOS silicon sensor as well as a Madatec IR 830 filter. Image processing was carried out in Adobe Lightroom 13.2 and Adobe Photoshop 25.3.1. A pure Egyptian blue tablet was included in the frame to obtain optimal image exposure.

FORS. Analysis was conducted using an Ocean Optics HR2000+ spectrophotometer, an Ocean Optics HL-2000-FHSA halogen lamp, and a Labsphere Spectralon Wavelength Calibration Standards white reference. The system includes two fiber optics, one single and one bifurcated, with a 400 μm diameter, equipped with an Ocean Optics RPH-2 anodized aluminum fiber support, enabling reflection measurements at a 90° or 45° angle to the bearing surface. Spectra were acquired in reflectance mode, within a 360–1000 nm spectral range, with $45^\circ/0^\circ$ optical geometry. Spectra were interpreted by comparison with published literature and spectral libraries available at the CCR scientific laboratories.

XRF. Analysis was performed using a Micro-EDXRF Bruker Artax 200 spectrometer (Milan, Italy) equipped with a fine focus X-ray source including a molybdenum anode and a Si(Li) silicon drift detector (SDD) with an 8 μm beryllium window, providing an average resolution of approximately 144 eV for the full width at half maximum of the manganese $K\alpha$ line. The system includes a 4096-channel analog-to-digital converter (ADC), a series of interchangeable filters, as well as two 0.65 mm and 1.5 mm collimators to adjust spot analysis size. Maximum voltage and current are 50 kV and 1500 μA , respectively, for a maximum power of 40 W. In the present case, measurements were carried out using 30-kV voltage, 1300 μA current, 60 s acquisition time, and a 1.5 mm collimator, with no filter, by fluxing helium gas onto the measurement area to improve the technique's detection limits (corresponding, with a helium flux, to $Z = 11$, sodium).

Raman. Analysis was carried out with a Bruker Bravo handheld spectrometer (Milan, Italy) equipped with a charge-coupled device (CCD) detector. Two lasers emitting light at 785 and 852 nm (Duo LASER™) were used as the excitation sources, enabling the acquisition of data in the $170\text{--}3200\text{ cm}^{-1}$ spectral range and at a spectral resolution of $10\text{--}12\text{ cm}^{-1}$. The output laser power was $\approx 50\text{ mW}$ for both lasers, while the number of scans and integration time were adjusted within the 2–20 and 300–2000-ms ranges, respectively, according to the color and Raman response of the different areas examined. With this system, spectral acquisition exploits a sequentially shifted excitation (SSE) algorithm that allows for automatic fluorescence removal. Spectra were interpreted by comparison with the published literature and spectral libraries available at the CCR scientific laboratories.

Micro-Raman. In only one instance, a microscopic sample of blue paint from Inv. 454 was analyzed using a benchtop dispersive Renishaw InVia Qontor system, coupled

with a Leica DM2700 microscope, available at the Raman Spectroscopy Laboratory of the Institute of Heritage Science of Italy's National Research Council (ISPC-CNR, Milan). This spectrometer is equipped with a Peltier-cooled NIR-enhanced CCD detector. Measurements were taken with 20× and 50× objectives, using 785 nm as the excitation wavelength. Spectra were acquired as a sum of 5–10 scans of 1–10 s in the 100–3200 cm^{-1} spectral range, with 1–2 cm^{-1} spectral resolution and 0.5–1 mW laser power at the sample.

FTIR. Analysis was conducted with a Bruker Vertex 70 FTIR spectrometer coupled with a Bruker Hyperion 3000 infrared microscope (Milan, Italy) and equipped with a mercury cadmium telluride (MCT) detector. Scrapings were analyzed as a bulk in transmission mode through a 15× objective, upon compression in a diamond cell. Data were collected in the 4000–650 cm^{-1} spectral range, at a spectral resolution of 4 cm^{-1} , as the sum of 64 scans. A cross section from Inv. 454 was analyzed in attenuated total reflection (ATR) mode using a 20× objective featuring a germanium crystal. Data were collected in the 4000–650 cm^{-1} spectral range, at a spectral resolution of 4 cm^{-1} , as the sum of 64 scans. Spectra were interpreted by comparison with the published literature and spectral libraries available at the CCR scientific laboratories.

Preparation of cross sections. Cross sections were prepared by embedding each multi-layered sample within a double layer of Struers EpoFix epoxy resin. After removal of the excess resin, the sample surface was finely polished using Struers abrasive cloths of progressively finer grits to expose the paint stratigraphy, thus enabling observation at high magnification and scientific analysis with various instrumental techniques.

Optical microscopy. Multi-layered samples were observed and photographed under visible light using an Olympus SZX10 stereomicroscope equipped with an Olympus Color View I digital camera (Segrate, Milan, Italy). After being mounted as cross sections, such samples were observed and photographed under visible and UV light using an Olympus BX51 minero-petrographic microscope equipped with an Olympus DP71 digital camera. In both cases, image acquisition and processing were performed with the analySIS FIVE 5.0 proprietary software.

SEM/EDS. Cross sections were observed and analyzed with a Zeiss EVO60 scanning electron microscope (Milan, Italy) equipped with a lanthanum hexaboride (LaB_6) cathode and an SDD, and coupled with a 40 mm^2 Oxford Ultim Max EDS microprobe for semi-quantitative elemental analysis. Samples were coated with a thin layer of carbon and analyzed in high vacuum mode using an accelerating voltage of 20 kV.

3. Results

The multi-analytical campaign described herein enabled the research team to collect an initial, yet relevant body of information regarding the materials and techniques used for the Chinese wooden sculptures' polychrome decoration, revealing precious aspects of their preservation state as well as transformation history from ritual items to collection artwork. The main observed issues that have hindered a full understanding of the artistic techniques to date include severe abrasion of some of the surfaces, combined with remarkable heterogeneity in terms of detected materials, noticeable discontinuity of the paint layers, and the lack of literature data from similar artifacts to compare our results with. The main outcomes gathered from this technical study, summarized in Table 1, are presented and discussed in detail in the following sections. In addition, a selection of representative data is shown in the Supplementary Materials file.

3.1. Identification of Paint Materials

3.1.1. Pigments and Dyes

Multiband imaging and non-invasive point analysis provided preliminary information on the presence, distribution, and identification of pigments and dyes on the objects' surface, either applied as part of the original decoration or within later interventions. As the outcomes of FORS, XRF, and Raman investigations were often not sufficient to deliver a detailed characterization of the polychromy in relation to the overall stratigraphy, multi-

layered samples were removed from select areas of interest, mounted as cross sections, and analyzed with optical microscopy and SEM/EDS. The main results obtained from this integrated approach are reported below.

Table 1. Summary of materials identified with scientific analysis. Summary of the main results obtained from scientific analysis of the seven polychrome wooden sculptures from MAO. For each sculpture, the number of samples removed is indicated, along with information on the ground layers, pigments and dyes found in the paint layers, binding media, and any other relevant materials detected. The [?] symbol indicates materials whose identification was uncertain, while the asterisk marks compounds ascribable to previous conservation treatments, including localized inpainting.

Sculptures	Samples Removed	Ground Layers	Pigments and Dyes in Paint Layers	Binding Media	Other Relevant Materials
<i>Arhat</i> <i>Inv. 448</i>	2 multi-layered 5 scrapings	Lithopone-based, additional presence of Si in innermost layer	Red Fe-containing pigments Minium Ultramarine blue * Prussian blue [traces] Green earth * Chrome green [traces] * Phthalocyanine green [traces]	[?]	Natural resin [?] * Acrylic resin * Alkyd resin
<i>Arhat</i> <i>Inv. 449</i>	4 multi-layered 8 scrapings	Lithopone-based, innermost layer with a calcium carbonate matrix and minor silicate inclusions	Red Fe-containing pigments Red lake (calcium carbonate substrate) Red lake (Al-silicate substrate) Minium Ultramarine blue Carbon-based black pigment * Phthalocyanine green	Oil [?] (Al and Zn stearates)	* PVAc
<i>Bodhisattva</i> <i>Inv. 450</i>	4 multi-layered 4 scrapings	Lithopone-based	Fe-containing earths Minium Red lake (calcium carbonate substrate) Red lake (Al- and Fe-silicate substrate) Carbon-based black pigment Ultramarine blue Mn- and Fe-containing blue pigment * Cd-, Cr-, Co-containing pigments [traces]	Oil	Rice starch Natural resin [?]
<i>Bodhisattva</i> <i>Inv. 451</i>	4 multi-layered 6 scrapings	Lithopone-based	Fe-containing earths Minium Red lake (Al- and Fe-silicate substrate) Carbon-based black pigment Ultramarine blue Mn- and Fe-containing blue pigment * Cd-, Cr-, Co-containing pigments [traces]	Oil	Rice starch Natural resin [?] * PVAc * Alkyd resin [traces]
<i>Buddha</i> <i>Inv. 452</i>	3 multi-layered 6 scrapings	Lithopone-based	Minium Fe-containing earths Ultramarine blue Mn- and Fe-containing blue pigment * Phthalocyanine blue	[?]	* PVAc

Table 1. Cont.

Sculptures	Samples Removed	Ground Layers	Pigments and Dyes in Paint Layers	Binding Media	Other Relevant Materials
<i>Guanyin</i> <i>Inv. 453</i>	3 multi-layered 9 scrapings	Lithopone-based	Fe-containing earths Ultramarine blue Carbon-based black pigment Minium * Organic brown glaze	Oil [?] (Al and Zn stearates)	Rice starch * Beeswax * PVAc * Alkyd resin [traces]
<i>Arhat</i> <i>Inv. 454</i>	6 multi-layered 8 scrapings	Lithopone-based	Titanium white Carbon-based black pigment Minium Phthalocyanine blue Red organic synthetic pigment	Alkyd resin	Rice starch * Acryl resin * PVAc [?]

- *Arhat—Inv. 448; Inv. 449*

The figure in *Inv. 448* wears a green garment covered with a red tunic that wraps around his entire body. Both clothing items show areas that are partly overpainted with different colors: for instance, green on certain regions of the tunic, especially on the legs' outer areas and lower drapery, which also displays local applications of blue paint, and blue over red on the garment edges. The bare skin, visible on the face and hands, has a dark red tone, while the hair is blue and appears shaved. The same color scheme, as well as various phases of locally applied repainting, are detected on *Inv. 449*, altogether similar to *Inv. 448* except for the lack of hair and a whitish flesh tone.

Cross sections from both sculptures show two to three light-colored paint applications above the wooden surface, possibly used as ground preparation, which in most cases are interposed with layers of color. These paints are based on lithopone, a white pigment first produced in the second half of the 19th century through co-precipitation of barium sulfate and zinc sulfide. In the samples examined, this material was sometimes mixed in with sparse grains of iron-containing earth pigments to convey a slight pink tone. For *Inv. 448*, elemental analysis revealed the additional presence of silicon in the innermost of these layers (Figure 2, left). The very first layer applied onto the wooden support of *Inv. 449*, on the other hand, displayed a different composition, consisting of a calcium carbonate matrix with minor silicate inclusions; this layer is followed, in the observed stratigraphy, by an intermediate iron-containing red paint and another lithopone ground layer (Figure S1, Supplementary Materials).

As far as red pigments are concerned, the flesh tones of *Inv. 448* are based on iron-containing earths; furthermore, minium was identified on details of the drapery, showing an orange–yellowish tone in IRFC. In *Inv. 449*, samples removed from the figure's face, right sleeve, and lower portion of the garment contain thin layers of organic red lakes within the stratigraphy, which are no longer visible on the surface due to numerous repainting campaigns (Figure 2, right). The presence of red lakes in the cross sections was detected through their distinctive UV-induced autofluorescence and by the absence of elements, in the EDS spectra, that could be deemed responsible for the layer coloration observed. SEM/EDS revealed the presence of calcium within these layers, suggesting that the dye might have been precipitated onto a calcium carbonate substrate to produce the lake pigment. In certain cases, this red lake was found in combination with either minium or an iron-containing red. Only in one sample, removed from an area of the *Arhat* below the right leg, the red colorant was precipitated onto an aluminum silicate type of substrate.

Ultramarine blue, which appears purple–red in IRFC, was the only blue pigment detected in *Inv. 448* on the *Arhat*'s hair and garment edges, also identified in one cross section from *Inv. 449*. Inner green layers are likely made of green earth, while the detection of copper with XRF and the typical dull dark blue color in IRFC suggest that the overpainting might be based on phthalocyanine green.

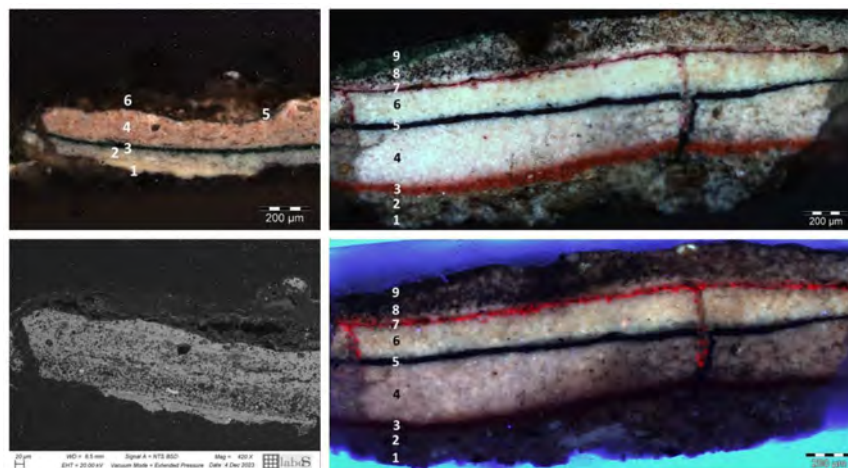


Figure 2. Paint stratigraphy, cross sections from Inv. 448 and 449. Polarized light (top left) and BSE (bottom left) images of a cross section from Inv. 448; the sequence of paint layers includes (1) lithopone with presence of silicon, (2) lithopone, (3) green earth with traces of chrome green, (4) lithopone with earth pigments, (5) ultramarine blue, and (6) organic layer. Polarized light (top right) and UV (bottom right) images of a cross section from Inv. 449; the sequence of paint layers includes (1) wooden support, (2) calcium carbonate with minor silicate inclusions, (3) earth pigments, (4) lithopone, (5) carbon-based black, (6) lithopone, (7) red lake with aluminum silicate substrate, (8) lithopone with traces of silicates, and (9) organic layer.

- *Bodhisattva—Inv. 450; Inv. 451*

Both figures, each dressed in a red garment covered with a red tunic with blue edges, sit on what looks like a green and brownish lotus flower; in both cases, losses in the superficial paint layer reveal an underlying blue color for the tunic, as well as red and blue tones for the lotus flower. Both figures show a cavity on their back of about 7–7.5 cm width × 14–15 cm height, perhaps used to collect offerings from devotees.

These two Bodhisattvas, which differ from one another only by a mirror gesture of their hands, present evident similarities also in terms of paint materials used for their polychrome decoration. Both sculptures contain one or two lithopone-based ground layers, often including scattered grains of earth pigments and minium. In all cases, the uppermost of these layers is applied onto an underlying layer of variable thickness, mostly consisting of minium. Visual examination of the microsamples with more complete stratigraphy shows that the minium paint is applied onto a lowermost layer based on lithopone with calcium carbonate inclusions. The complete layer structure would, therefore, include a minium layer sandwiched between two lithopone layers (Figure 3 and Figure S1, Supplementary Materials).

Flesh tones are obtained as mixtures of lithopone, iron-containing earths, and minium. XRF data highlight the use of earth pigments also in the two figures' garments. Red lakes were identified either on the objects' surface or within the stratigraphy, making them no longer visible in the latter instance. SEM/EDS analysis of an inner layer in a single sample from Inv. 450 indicated that the organic red dye was likely precipitated onto a calcium carbonate substrate; in all other cases, the inorganic substrate used for the lake preparation is based on aluminum and iron-rich silicates. When these lakes were found on the sculptures' surface, as in the present case, their nature could be further investigated by FORS: the results suggested the use of a dye of animal origin, likely obtained from scale insects of the Coccidae family (Figure 3).

The colorful paint stratigraphy of the two Bodhisattvas was found to also include carbon-based black and ultramarine blue layers. While the latter is typically associated with a purple–red color in IRFC, another blue pigment with a dark blue tone in IRFC was extensively detected for later repainting both in Inv. 450 and Inv. 451, mainly located on the figures' hair and blue details of their garments. XRF analysis revealed the presence

of manganese and iron, although the exact pigment currently remains unidentified. The chemical composition of the green pigments also eluded non-invasive point analysis. The surface of both sculptures showed limited retouching, where cadmium-, cobalt-, and chromium-rich pigments of industrial production were found.

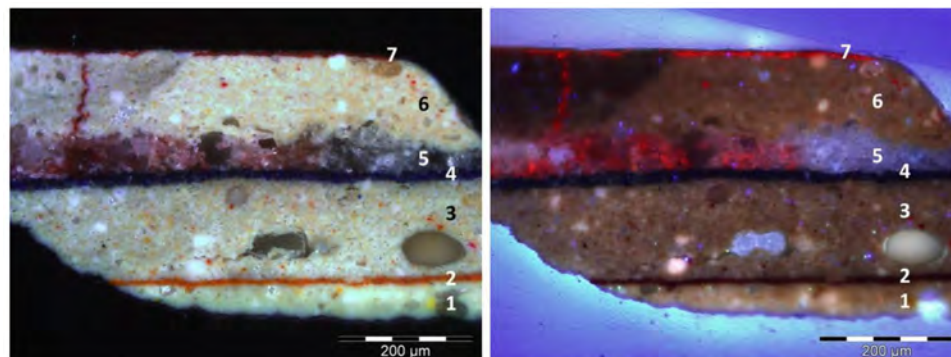


Figure 3. Paint stratigraphy, cross section from Inv. 450. Polarized light (left) and UV (right) images of a cross section from Inv. 450; the sequence of paint layers includes (1) lithopone with sparse calcium carbonate inclusions and earth pigments, (2) minium, (3) lithopone with sparse earth pigments, (4) ultramarine blue, (5) red lake with calcium carbonate substrate, (6) lithopone with sparse earth pigments, and (7) red lake with aluminum and iron silicate substrate.

Finally, a close inspection of the polychrome decoration highlighted the presence, in some areas, of canvas underneath the paint layers, possibly added in both sculptures to join different wooden blocks or to repair existing fractures.

- *Buddha—Inv. 452*

Inv. 452 is a Buddha sitting in meditation posture, with crossed legs and clasped hands, corresponding to the so-called lotus position. The figure is wearing a green garment covered with draperies: two are used for the body, one red and one blue, and one for the legs, of a dark blue tone. His hair is shaped into regular rows of curls, painted blue according to the Chinese iconographic tradition. A smooth ovoid-shaped protuberance is located halfway between the forehead and the top of the head. The center of the forehead currently displays a hole, where perhaps a semi-precious stone or glass ornament was originally placed to mark the figure's "third eye", now missing. As in the case of Inv. 450 and 451, a cavity of about 10.5 cm width \times 25 cm height is located on the Buddha's back, likely intended for devotees to place offerings.

The multi-analytical protocol adopted in this study proved particularly useful to shed light on the peculiar technique used to create this Buddha's hairstyle: the volume appears to have been obtained by modeling clay mixtures, which were then painted with ultramarine blue; the presence of an intermediate ground containing lithopone was revealed by optical microscopy and SEM/EDS analysis of the cross sections.

Compared to the other sculptures under study, the variety of pigments and number of overlapping paint layers found in Inv. 452 are limited. In samples removed from both the flesh tones and garment, a lowermost grayish lithopone-based ground layer is followed by a thin layer of minium and one or two additional layers containing primarily lithopone with scattered grains of earth pigments or ultramarine blue. Flesh tones, indeed, were obtained by mixing lithopone with minium. The Buddha's red garment is made of a thick single layer of minium mixed in with iron-containing pigments, jointly yielding an overall orange–greenish color in IRFC. Similarly to Bodhisattvas Inv. 450 and Inv. 451, the drapery's blue pigment, appearing dark blue in IRFC and containing both manganese and iron, could not be identified conclusively. Multiband imaging suggested the presence of extensive retouching on the figure's back: based on the XRF identification of copper and IRFC data, it is possible to hypothesize the use of phthalocyanine blue.

As in the case of Inv. 450 and 451, careful observation of the surface revealed the presence of at least two types of canvas underneath the polychrome decoration in some areas of this sculpture.

- *Guanyin—Inv. 453*

Inv. 453 is limply lying on a support shaped in the form of a perforated rock, with the body slightly twisted to the right and the face oriented frontally. The figure is dressed in a brownish-colored robe covered with a blue drapery, which leaves parts of the pink torso and arms exposed. The hair is styled conventionally, with large locks extending to the shoulders. The hair bun at the top of the head is adorned frontally by a tripartite tiara, while the chest and arms are embellished with jewels.

Among the seven pieces examined in this study, this sculpture shows the most complex paint stratigraphy, with each layer obtained as a mixture of various pigments. At least four ground layers are present, with lithopone mixed in with very fine grains of ultramarine blue, as well as yellow and red iron-containing pigments. In the cross sections, these layers are located in between other colored layers, namely a red layer made of an iron-based pigment, an organic black, and ultramarine blue (Figure 4).

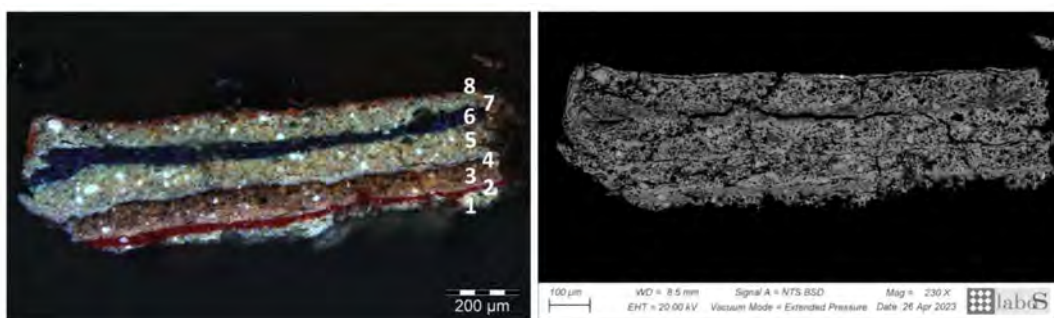


Figure 4. Paint stratigraphy, cross section from Inv. 453. Polarized light (left) and BSE (right) images of a cross section from Inv. 453; the sequence of paint layers includes (1) lithopone with sparse earth pigments and ultramarine blue, (2) earth pigments, (3) lithopone with sparse earth pigments and ultramarine blue, (4) carbon-based black, (5) lithopone with sparse calcium carbonate inclusions and earth pigments, (6) ultramarine blue, (7) lithopone with sparse earth pigments, and (8) minium.

Based on FORS data, the use of a mixture of earth pigments and red lake in the flesh tones may not be ruled out (Figure S2, Supplementary Materials). Only in one sample removed from the red drapery and examined by SEM/EDS, minium was applied to the surface as an extremely thin layer.

Close inspection of the artifact, along with the outcomes of laser cleaning testing carried out in a second phase of this project, suggested the presence of a thin brown layer, presumably of organic nature, used as a superficial glaze. As for Inv. 450, 451, and 452, a canvas layer is visible underneath the paint layers in some areas of the Guanyin.

- *Arhat—Inv. 454*

Inv. 454 represents a monk with white skin, wearing a greenish garment covered with a red tunic while sitting on a wooden trunk with crossed legs. Close inspection of this sculpture reveals a complex layering of materials, generally of the same color, especially for the tunic and skin, the latter heavily retouched in a recent intervention. No overpainting appears to be present for the green garment upon visual examination.

Since the onset of this research, Inv. 454 has raised the most questions: from an iconographic point of view, some features appear unusual, such as the garment's cut, revealing the figure's breast, and the proportions of the light blue–greenish drapery in the lower part of the sculpture, which looks stiff and overly elongated. The presence of a square-shaped cavity of about 6 cm width × 6.5 cm height on the figure's back posed an additional challenge: indeed, the current interpretation of these cavities as places originally

used to collect devotees' offerings applies to sculptures depicting Buddha or Bodhisattvas, but would be unusual for a monk.

At least two lithopone-based white layers are present within the stratigraphy in the cross sections examined, separated by two very thin adjacent layers, one appearing as a black organic layer and the other as a discontinuous layer of minium. In two out of four samples analyzed by optical microscopy and SEM/EDS, an additional innermost thin minium layer was applied directly onto the wooden support. A sample removed from the light blue–greenish drapery stands out due to the absence of minium (Figure 5, right). In all cases, a titanium-rich white thin layer is present on top of the outer preparation, which also matches the composition of the white flesh tone. Phthalocyanine blue, along with anatase and barite, was identified in a sample from the drapery with micro-Raman analysis (Figure S3a, Supplementary Materials). The red pigment used for the garment could not be unambiguously characterized, although FTIR measurements suggested the presence of an organic synthetic pigment. Portable Raman analysis of a paint loss on the figure's red garment, revealing another red color underneath, detected the presence of an underlayer based on minium and gypsum. Measurements conducted on other color fields, including various shades of blue on the garment, the green hue of the waistband, and a red tone on the elbow's outer part, only yielded the typical signals of anatase and barite (Figure S3b, Supplementary Materials).

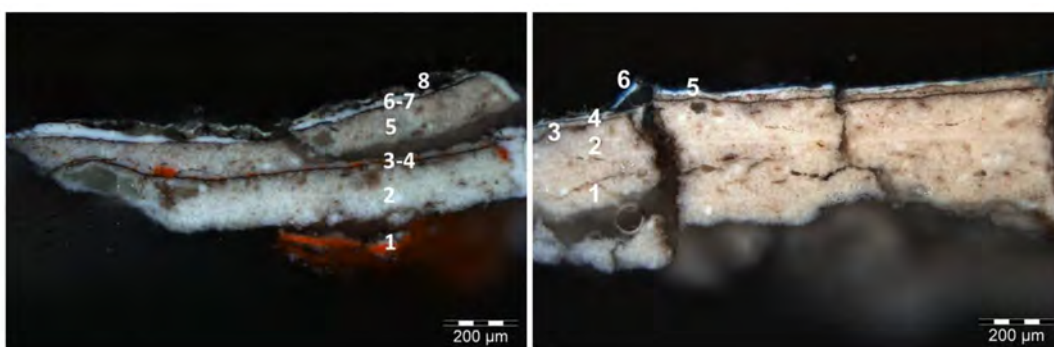


Figure 5. Paint stratigraphy, cross sections from Inv. 454. Polarized light images of cross sections from Inv. 454; the sequence of paint layers includes at (left) (1) minium, (2) lithopone, (3) carbon-based black, (4) minium, (5) lithopone, (6) carbon-based black, (7) lithopone and titanium white, and (8) organic layer; at (right) (1) lithopone, (2) lithopone with sparse earth pigments, (3) carbon-based black, (4) lithopone, (5) titanium white, and (6) titanium white and phthalocyanine blue.

3.1.2. Binding Media and Other Organic Materials

FTIR analysis of the microscopic scrapings provided hints as to the identification of binding media and synthetic organic materials in the sculptures' current polychrome decoration. A selection of spectra showing the presence of different classes of binders and other organic substances detected is shown in Figure S4, Supplementary Materials.

The presence of oil was detected in Bodhisattvas Inv. 450 and 451. The same material was found in Arhat Inv. 449 and Guanyin Inv. 453, where zinc and aluminum stearates were also identified as possible additives from industrial paint tube colors. A limited presence of natural resin or oleoresin cannot be ruled out in these three artifacts based on the data collected. Moreover, beeswax was detected as a final coating in a scraping removed from the left knee of Guanyin Inv. 453, interpreted as a brownish finish applied in the past to minimize a particularly fragmentary aspect of the surface while mimicking the appearance of a monochrome object.

Polyvinyl acetate was found in samples from Inv. 449, 451, 452, and 453, and its presence was also hypothesized for Inv. 454; this material, which appears to have penetrated the paint layers, was likely applied within later interventions. The presence of acrylic and alkyd resins, used individually or together, was identified in samples from Inv. 448; alkyd resins may have been used in Inv. 451 and 453 as well.

As regards Arhat Inv. 454, the main binding medium detected in the polychrome decoration was alkyd resin, although acrylic resin and polyvinyl acetate were also found, possibly used as conservation materials.

3.1.3. The Finding of Starch Lumps

SEM investigation of the cross sections removed from Inv. 454 highlighted the presence of organic lumps with rounded to irregular shapes within the stratigraphy, most of which are embedded in the lithopone-based ground layers. These lumps, showing variable sizes (30–120 μm width \times 10–50 μm height), consist of aggregates of polyhedral granules of about 3 μm diameter. Micro-ATR-FTIR analysis identified this material as starch; according to the literature [20–22], the observed granule size is most compatible with rice starch, normally falling into the 2–7 μm range (Figure 6). The abundance and distribution of these starch lumps suggest that they might have been added intentionally, although different hypotheses on their purpose may be entertained. Finally, examining the SEM images collected from the cross sections of all seven sculptures, the presence of rice starch lumps was also hypothesized for Bodhisattvas Inv. 450 and 451, and for Guanyin Inv. 453, based on morphological data. However, in these three sculptures, the aggregates typically have smaller sizes than in Inv. 454.

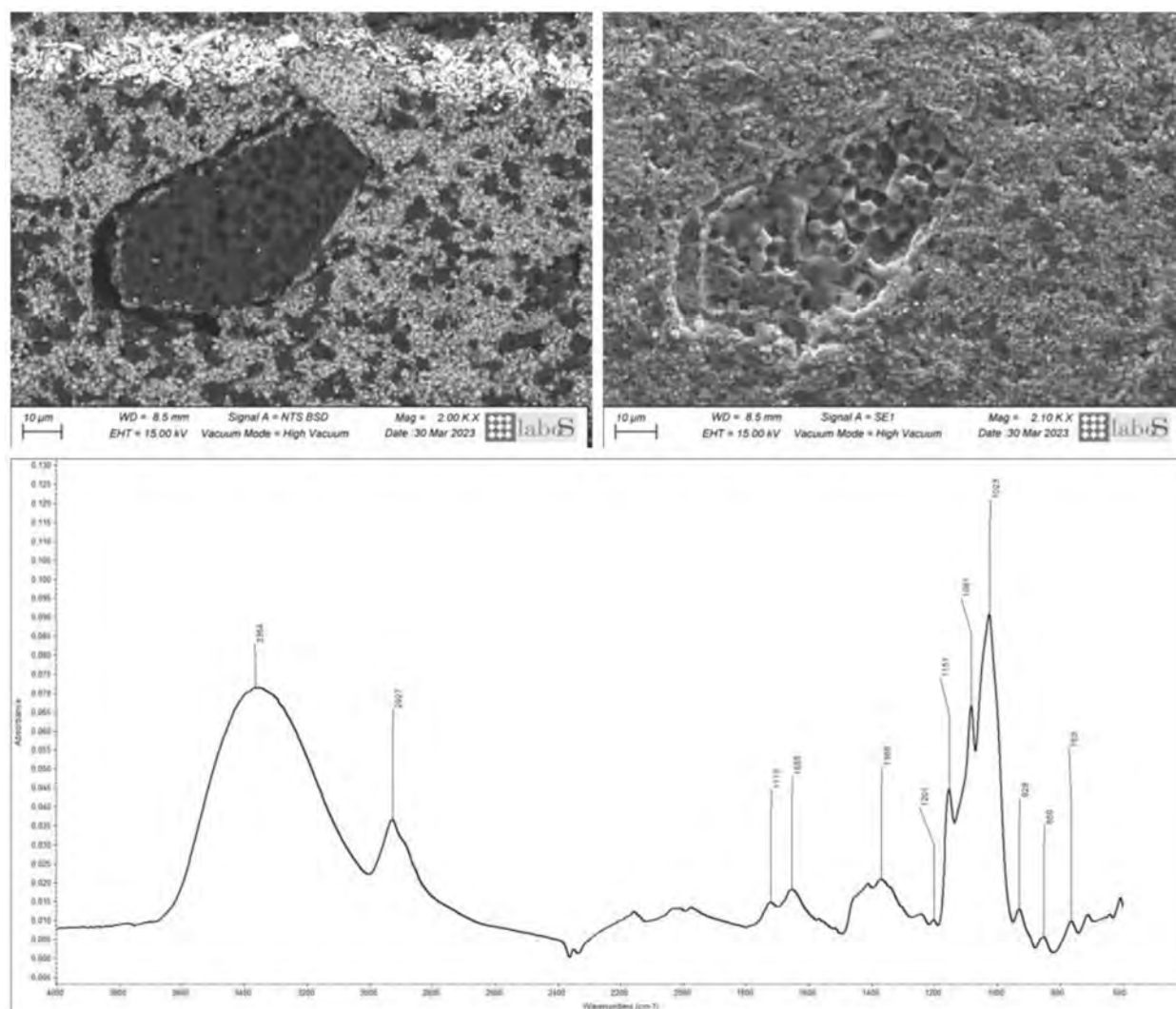


Figure 6. Starch lumps. BSE and SE images of a starch lump as found in a cross section from Inv. 454 (top); micro-ATR-FTIR spectrum of the starch lump (bottom).

3.2. Conservation Issues

Aside from widespread dust deposits, all seven sculptures displayed an untidy appearance before treatment due to the sequential application of multiple materials over time and to a fragmented condition that particularly concerned the uppermost paint layer. Moreover, significant embrittlement of the wooden structure and the entire decoration was observed in combination with frequent paint cracking (Figure 7). Scientific analysis, especially optical and electron microscopy, was key to highlighting issues related to the presence of biodeteriogenic microorganisms and structural degradation of the paint.

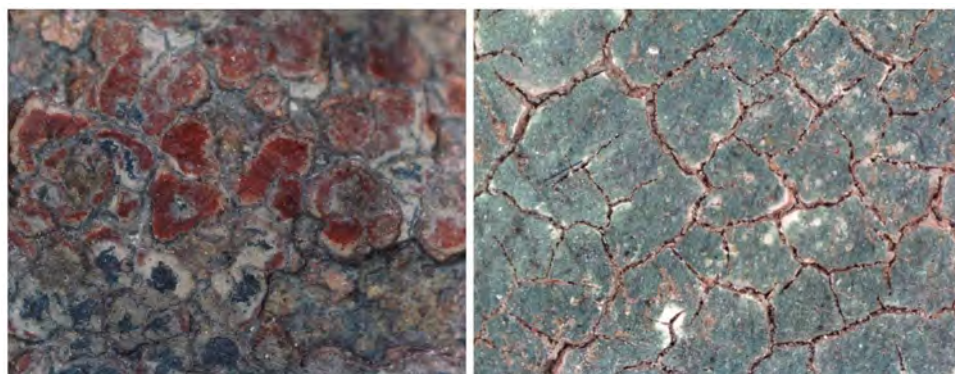


Figure 7. Surface condition. Microphotographs of the surface condition in Inv. 450 (left) and Inv. 449 (right), showing multiple layers of polychromy and severe paint cracking.

In particular, examination of the cross sections from Arhat Inv. 449 via optical microscope revealed a former growth of micro-colonial fungi, which penetrated the lithopone-based ground layers (Figure 8, left). Moreover, the joint presence of hyphae from different fungal species was detected within the same layers by means of SEM: the hyphae were identified in the backscattered electron (BSE) images by their rounded transversal sections, showing 10–15 μm diameter (Figure 8, middle). Similar hyphae transversal sections, although less numerous and dense, were also observed in Bodhisattvas Inv. 450 and 451, Buddha Inv. 452, and Guanyin Inv. 453.

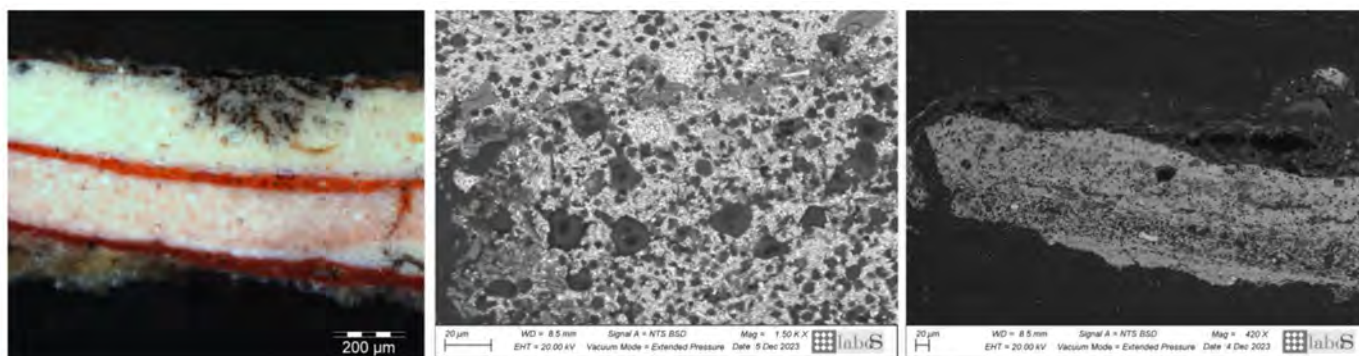


Figure 8. Microbiological colonization. Polarized light (left) and BSE (middle and right) images of cross sections from Inv. 449 (left and middle) and 448 (right), showing a growth of micro-colonial fungi (left) and the transversal sections of hyphae from different fungal species (middle and right).

SEM analysis of the available cross sections shed light on another distinctive feature of the paint stratigraphy that appears to be common to all the sculptures investigated, except for Buddha Inv. 452: all the lithopone-based grounds found in the samples from Arhats Inv. 449 and Inv. 454, as well as Guanyin Inv. 453, display widespread black rounded dots with an average size of 2–5 μm in BSE mode. Careful inspection in BSE and secondary electron (SE) modes did not clarify whether this pattern might be due to a dense distribution of pores that are now filled with epoxy resin as a result of cross section

preparation or with an organic substance from the paint formulation. The observed dotted pattern does not appear to be consistent with a distribution of single rice starch granules, which would display a polyhedral shape instead (Figure 6). The same feature is observed in other cases as well, including Arhat Inv. 448 and Bodhisattvas Inv. 450 and 451, for which the dot density seems to decrease from the inner to the outer portion of the layer. It is worth noting that the innermost lithopone layers with the additional presence of silicon (Inv. 448) or calcium carbonate inclusions (Inv. 450 and 451) do not show such a pattern. The considerations above suggest that this feature is likely due to a deterioration process, possibly of a biological nature, which might have determined a considerable depletion in binder. This might justify the extremely fragile condition of the paint layers, observed for all the sculptures and particularly evident in the cross sections from Inv. 453. The sequential application of many superimposed layers of paint, presumably occurring over a few decades, might be related to an attempt to remedy the ongoing deterioration process. This may also explain the decreasing porosity of the outer lithopone layers in Inv. 448, 450, and 451, which, after repainting, underwent deterioration again (Figure 8, right). In this context, the presence of polyvinyl acetate and acrylic resins, detected by FTIR down to the inner layers of the sculptures' decoration, might be related to the use of consolidants and adhesives as a treatment for the observed porosity.

4. Discussion

The presence of lithopone-based ground layers in all the sculptures analyzed is in contrast with dating hypotheses initially formulated by experts based on stylistic considerations and a comparison of the carving techniques, which placed the objects before the 19th century. A careful review of the results of this study, and particularly the widespread identification of lithopone in the lowermost layers of the cross sections, suggests that, while the sculptures appear to retain an original wooden body, a complete refurbishment of their polychrome decoration may have occurred sometime after they were first created. This interpretation is further corroborated by an in-depth examination of their fabrication techniques based on data from computed tomography, which will be the subject of a forthcoming publication. The repainting and refurbishment of sculptures are documented as common practices in ancient China and during the Qing dynasty [9–11,14,19].

While lithopone-based ground layers were likely applied as part of the sculptures' repainting campaigns, the detection of trace remnants of a calcium carbonate layer in a cross section from Inv. 449 may provide clues as to the presence of a more ancient, possibly original decoration. This finding is consistent with data from previous studies in the literature [23], in which calcite, along with lead white, is reported to be one of the materials most commonly used for white grounds, especially on Buddhist clay sculptures and wall paintings. However, the almost complete lack of material in the cross sections examined suggests that this former, possibly original decoration was completely stripped at some point in time prior to the repainting campaigns.

The use of iron-based and lead-based red pigments such as red earth and minium, ubiquitous in the samples examined, is well documented in Chinese painted productions. As revealed by historical records and ancient Chinese building construction manuals [24,25], the sculptures' polychrome decoration shows interesting similarities with the architectural painting practice of the Qing dynasty. Among these, it is worth mentioning the detection of red pigments, such as iron oxides, as underlayers in some of the architectural elements of the Fushan Temple's Bell and Drum Towers in China's Shaanxi Province [24]. Further information about the layering of colors as a typical technical feature of Chinese painting in the Shaanxi region is provided elsewhere [25]. The use of minium as an underlayer in painted clay sculptures from Northern China was reported in a previous work [10]: in that case, two overlapping layers, blue and red, respectively, were found in a cross section, each composed of a paper ground layer with pigments applied onto it. The practice of repainting sculptures with several layers of painted paper to cover the previous damaged decoration is reported for both the Ming and Qing dynasties [9]. As for the blue pigments,

ultramarine blue was identified in all the samples examined in this work, its use being documented in China since antiquity [7,8].

Another interesting outcome of the present study is the identification of red lakes produced by precipitating an organic colorant of animal origin onto two different inorganic substrates: calcium carbonate or aluminum- and iron-rich silicates. Both lakes were identified in cross sections from Inv. 449 and 451, suggesting that these repainting may have occurred at different times or within distinct campaigns. Only the second type of red lake, with an aluminum and iron silicate substrate, was found in Inv. 451.

Among the materials identified, a brown paint layer observed in historical photographs for Inv. 450, 451, 452, and 453 appears to have been summarily removed during previous treatments. This layer may be interpreted as an attempt to adapt the decoration's tone to the taste of 20th-century European collectors. This common element suggests that these four sculptures likely underwent similar processes upon their arrival in Europe. In addition, a brownish organic layer found on Inv. 453, which is neither original nor a Western pseudo-lacquer, was probably applied as a superficial glaze upon removal of the monochrome brown paint to soften the perceived visual contrast resulting from the presence of numerous paint losses in the polychrome decoration. This glaze is indicative of a specific European taste that, in line with the dictates of the Italian conservation discipline, is constantly seeking an overall chromatic balance.

Overall, scientific analysis revealed a similar color palette for all the sculptures analyzed, except for Arhat Inv. 454. This was the only artifact to include titanium white, phthalocyanine blue, and a red organic synthetic pigment, all dispersed in alkyd resin, which indicates that the painted decoration was applied no earlier than the 1930s. These elements point to a different history compared to the other artifacts, either traceable to the sculpture's transfer from China to Europe or, at least, related to a heavier paint makeover.

Buddha Inv. 452 displays a series of distinctive features compared to the rest of the group: on the one hand, it has a significantly simpler polychrome decoration, with fewer overlapping paint layers; on the other, it is the only artifact whose lithopone-based ground layers are not affected by porosity-related deterioration, which may be ascribable to a different conservation history prior to its acquisition by the MAO.

The presence of starch lumps within the lithopone-based ground layers, as well as the interpretation of their intended purpose, prompted careful thinking: as a first consideration, the abundance of these lumps within the layers suggests that they may have been added intentionally to the paint formulation. The use of starch is documented, for instance, in an ancient Chinese building construction manual, entitled "*Gongcheng Zuofa Zeli*" [26], when referring to the current practices of the Qing dynasty (1636–1912 C.E.). According to this manual, starch, in the form of flour, was commonly mixed with other ingredients within the ground layer of architectural paintings [24]. Moreover, starch-based yellow pigments have been detected in mixtures for red, white, blue, green, and yellow colors from the Tibetan Buddhist Monastery of Puren, China [27]. As for Inv. 454, the larger size and more regular shape of the starch lumps more evidently indicate a deliberate addition, perhaps aiming to prompt cracking of the paint layers in an attempt to simulate an ancient appearance for this sculpture through induced degradation of its surface decoration. This property of starch, enabled by its hygroscopic behavior, is mentioned in the literature with regard to forgery techniques [28,29].

In summary, the seven sculptures examined showed multiple layers of polychromy, indicating extensive repainting and changes in design over time, which may have been carried out to repair particularly degraded paint conditions at various points in their history for ritual use, or to facilitate their sale on the European art market. The overall homogeneity of the current paint layers suggests that the original decoration was likely removed prior to the repainting campaigns. Based on the paint materials identified, it is not possible to ascertain whether the repainting might have been completed in China or if some of it may have occurred after the sculptures were transferred to Europe as well.

5. Conclusions

The technical study presented herein aims to fill in the gaps regarding the materials and techniques of ancient Chinese painting, especially in relation to the production of Buddhist polychrome wooden sculptures. As the objects examined have different provenance and dating, striking similarities were detected, for instance, in terms of deterioration and microbiological colonization that appear to indicate a common conservation history at least from a specific point in time onward.

Scientific analysis of the polychrome decoration, combined with a thorough examination of numerous paint cross sections with optical and electron microscopy, suggest that the sculptures were completely repainted upon removal of the former, possibly original decoration. Possible reasons for these repainting campaigns include an intention to remedy ongoing paint degradation phenomena and an attempt to adapt their appearance to Western taste, thus facilitating their sale on the European art market. Further details on the sculptures' fabrication techniques and assembly from multiple wooden elements will be shared as part of a forthcoming publication, along with a discussion of the most relevant implications in terms of dating and authenticity.

Supplementary Materials: The following supporting information can be downloaded at <https://www.mdpi.com/article/10.3390/coatings14030344/s1>, Figure S1: Representative EDS spectra; Figure S2: Representative FORS spectra; Figure S3: Representative Raman spectra; Figure S4: Representative FTIR spectra.

Author Contributions: Conceptualization, C.R., P.B. and F.P.; methodology, C.R. and F.P.; scientific analysis, C.R., A.P., D.A., F.P., D.D. and F.D.I.; data interpretation, C.R., P.B., F.P., D.A., A.P., E.M., V.T., N.S., F.Z., S.C., L.V. and D.Q.; writing—original draft preparation, C.R., P.B. and F.P.; writing—review and editing, C.R., P.B. and F.P.; supervision, F.P.; funding acquisition, D.Q. All authors have read and agreed to the published version of the manuscript.

Funding: This research was funded by the Museo d'Arte Orientale (MAO).

Institutional Review Board Statement: Not applicable.

Informed Consent Statement: Not applicable.

Data Availability Statement: All data generated during this study are either included in this published article or available from the corresponding author upon reasonable request.

Acknowledgments: We would like to dedicate this article to our dear friend and colleague Debora Angelici, who passed away prematurely in June 2023. We are grateful to the Raman Spectroscopy Laboratory, Institute of Heritage Science of Italy's National Research Council (ISPC-CNR, Milan) for analyzing one sample with micro-Raman spectroscopy. We would also like to acknowledge Paola Manchinu and Michela Cardinali, CCR "La Venaria Reale", for supporting this research.

Conflicts of Interest: The authors declare no conflicts of interest.

References

1. Steineck, T.I. Research and Evaluation of Japanese Buddhist Objects in European Museum: Lessons of a Digitalization Project. 2015.
2. Mertz, M.; Itoh, T. The Study of Buddhist Sculptures from Japan and China Based on Wood Identification. In *Scientific Research on the Sculptural Arts of Asia Proceedings of the Third Forbes Symposium at the Freer Gallery of Art*; Archetype Publications in association with the Freer Gallery of Art; Smithsonian Institution: Washington, DC, USA, 2007; Volume 3, pp. 198–204.
3. Richter, M. Three Polychrome Japanese Buddhist Sculptures from the Kamakura Period: The Scientific Examination of Layer Structures, Ground Materials, Pigments, Metal Leafs, and Powders. In *Scientific Research on the Pictorial Arts of Asia—Proceedings of the Second Forbes Symposium at the Freer Gallery of Art*; Archetype Publications Ltd.: London, UK, 2005; pp. 21–34.
4. Richter, M. Two Thirteenth-Century Polychrome Sculptures in Shomyo-ji and Ensho-ji. In *Historische Polychromie. Skulpturenfassung in Deutschland und Japan Historical Polychromy. Polychrome Sculpture in Germany and Japan*; Hirmer Verlag: München, Germany, 2004.
5. Yamasaki, K.; Nishikawa, K. Polychromed sculptures in Japan. *Stud. Conserv.* **1970**, *15*, 278–293.
6. Miura, S. Polychromie in Japan: Eine chronologische Zusammenstellung der Malmaterialien. Polychromy in Japan: A chronological compilation of artists' materials. In *Historische Polychromie: Skulpturenfassung in Deutschland und Japan*; Hirmer: Munich, Germany, 2004; pp. 244–250.

7. Song, Y.; Zhou, L.; Wang, Y.; Liu, F.; Guo, J.; Wang, R.; Nevin, A. Technical study of the paint layers from buddhist sculptures unearthed from the longxing temple site in Qingzhou, China. *Heritage* **2021**, *4*, 2599–2622. [[CrossRef](#)]
8. Song, J.; Xiang, W.; Yan, S.; Zhou, W.; Ma, L. Craftsmanship and materials: Painted Bodhisattva sculptures in the Fengguo Temple dated to the year 1020 in Yi County, Northeast China. *Herit. Sci.* **2021**, *9*, 1–19. [[CrossRef](#)]
9. Bai, X.; Jia, C.; Chen, Z.; Gong, Y.; Cheng, H.; Wang, J. Analytical study of Buddha sculptures in Jingyin temple of Taiyuan, China. *Herit. Sci.* **2021**, *9*, 1–19. [[CrossRef](#)]
10. Bai, X.; Xia, H.; Wang, R.; Fan, W.; Shi, M.; Liu, Q.; Xie, Y. Study on the Painted Clay Sculptures of Ming Dynasty in Jingyin Temple of Taiyuan, China. 2022.
11. Shen, J.; Li, L.; Zhang, D.; Dong, S.; Xiang, J.; Xu, N. A Multi-Analytical Approach to Investigate the Polychrome Clay Sculpture in Qinglian Temple of Jincheng, China. *Materials* **2022**, *15*, 5470. [[CrossRef](#)] [[PubMed](#)]
12. Jett, P.J.; Douglas, J.G. Chinese Buddhist bronzes in the Freer Gallery of Art: Physical features and elemental composition. *MRS Online Proc. Libr.* **1992**, *267*, 205–223.
13. Chloros, J. Technical Study of an 11th–12th Century Guanyin Sculpture. 2023. Available online: <https://www.gardnermuseum.org/blog/technical-study-11th-12th-century-guanyin-sculpture> (accessed on 1 February 2024).
14. Twilley, J.; Garland, K.M. The redecoration history of a Chinese polychromed Guanyin attributed to the 11th–12th century CE as deduced from stratigraphic microanalysis. *MRS Online Proc. Libr. (OPL)* **2011**, *1319*, mrsf10-1319.
15. Webb, M.; Moffatt, E.; Corbeil, M.C.; Duxin, N. Examination and Analysis of the Chinese Polychrome Sculptures in the Collection of the Royal Ontario Museum in Scientific Research on the Sculptural Arts of Asia. In Proceedings of the Third Forbes Symposium at the Freer Gallery of Art; Douglas, J.G., Jett, P., Winter, J., Eds.; Archetype: London, UK, 2007; pp. 188–197.
16. Scott, R.E. Larson John and Kerr Rose: Guanyin: A masterpiece revealed. 73 pp. London: Victoria and Albert Museum, 1985. *Bull. Sch. Orient. Afr. Stud.* **1989**, *52*, 186. [[CrossRef](#)]
17. Larson, J.H. The treatment and examination of polychrome Chinese sculpture at the Victoria and Albert Museum. *Stud. Conserv.* **1988**, *33*, 120–125. [[CrossRef](#)]
18. Lorne, A.; Rösch, P. The Chinese wooden sculpture of Guanyin: New technical and art historical insights. *Bull. Van Het Rijksmus.* **2002**, *50*, 364–389.
19. Leidy, D.P.; Strahan, D.K. *Wisdom Embodied: Chinese Buddhist and Daoist Sculpture in the Metropolitan Museum of Art*; Metropolitan Museum of Art: New York, NY, USA, 2010.
20. Kasem, S.; Waters DL, E.; Rice, N.F.; Shapter, F.M.; Henry, R.J. The endosperm morphology of rice and its wild relatives as observed by scanning electron microscopy. *Rice* **2011**, *4*, 12–20. [[CrossRef](#)]
21. Yu, H.H.; Lee, Y.; Nam, Y.S.; Kim, M.H.; Lee, K.B.; Lee, Y. Surface Analysis of Fermented Wheat and Rice Starch Used for Coating Traditional Korean Textiles. *Materials* **2022**, *15*, 2001. [[CrossRef](#)] [[PubMed](#)]
22. Ramos, A.H.; Rockenbach, B.A.; Ferreira, C.D.; Gutkoski, L.C.; de Oliveira, M. Characteristics of flour and starch isolated from red rice subjected to different drying conditions. *Starch-Stärke* **2019**, *71*, 1800257. [[CrossRef](#)]
23. Gao, Y.; Yang, Q.; Sun, M.; Zhen, G.; Zhang, F. Study of the pigments of sculptures in Shuilu Temple. *Sci. Conserv. Archaeol* **2022**, *64*, 97–108.
24. Zou, W.; Yeo, S.Y. Investigation on the Painting Materials and Profile Structures Used in Ancient Chinese Folk Architectural Paintings by Multiple Analytical Methods. *Coatings* **2022**, *12*, 320. [[CrossRef](#)]
25. Egel, E.; Simon, S. Investigation of the painting materials in Zhongshan Grottoes (Shaanxi, China). *Herit. Sci.* **2013**, *1*, 1–12. [[CrossRef](#)]
26. Liang, S.C. *Qing-Dynasty Municipal Engineering*; Tsinghua University Press: Beijing, China, 2006.
27. Teri, G.; Han, K.; Huang, D.; Li, Y.; Tian, Y.; Chao, X.; Li, Y. A Study on the Materials Used in the Ancient Architectural Paintings from the Qing Dynasty Tibetan Buddhist Monastery of Puren, China. *Materials* **2023**, *16*, 6404. [[CrossRef](#)] [[PubMed](#)]
28. Broers, N. *Scientific Investigation of Copies, Fakes and Forgeries*; Craddock, P., Ed.; CeROArt. Conservation, exposition, Restauration d’Objets d’Art (No. EGG 1); Association CeROArt asbl; Butterworth-Heinemann: Oxford, UK, 2009; pp. 306–307.
29. Fong, W. The problem of forgeries in Chinese painting. Part one. *Artibus Asiae* **1962**, *25*, 95–140. [[CrossRef](#)]

Disclaimer/Publisher’s Note: The statements, opinions and data contained in all publications are solely those of the individual author(s) and contributor(s) and not of MDPI and/or the editor(s). MDPI and/or the editor(s) disclaim responsibility for any injury to people or property resulting from any ideas, methods, instructions or products referred to in the content.